A cylindrical self-consistent modelling of vegetal wools thermal conductivity

Clément Piegay, Philippe Gle, Emmanuel Gourdon, Etienne Gourlay

A cylindrical self-consistent modelling of vegetal wools thermal conductivity

Clément Piegay, Philippe Gle, Emmanuel Gourdon, Etienne Gourlay

A cylindrical self-consistent modelling of vegetal wools thermal conductivity

Clément Piégay [a,b,c,*], Philippe Glé [a], Emmanuel Gourdon [c], Etienne Gourlay [b]

[a] Cerema, Ifsttar, UMRAE – Laboratoire de Strasbourg, 11 rue Jean Mentelin, 67035 Strasbourg, France
[b] Cerema, BPE Team – Laboratoire de Strasbourg, 11 rue Jean Mentelin, 67035 Strasbourg, France
[c] Université de Lyon, ENTPE, LTDS UMR CNRS 5513, 3 rue Maurice Audin, 69518 Vaulx-en-Velin Cedex, France

In recent years, the fight against climate change has come to the fore. In this scope, the use of vegetal wools, which can store carbon dioxide, is particularly relevant for developing greenbuilding solutions. Moreover, considering their high porosity levels, the thermal performances of these materials can com-pete with conventional insulators ones. These performances are related to the microscale vegetal fibres specificities that are used in the wool manufacturing process. So, a self-consistent modelling approach is developed in order to model the vegetal wools thermal properties as a function of their microscale parameters. To do that, a simplifying assumption assimilates the fibres to a representative elementary volume based on a biphasic (including solid and fluid phases) cylindrical inclusion. This model has been validated in the specific case of a flow perpendicular to the fibres by comparison with experimental char-acterisations performed on four materials in real hygrothermal conditions and with data from literature. Thanks to a parametric analysis, it is finally shown that for high porosity values ($> 95\%$), vegetal wools thermal properties present interesting values regardless of the solid phase thermal conductivity.

1. Introduction

In the actuel context of climate change awareness, the building sector appears to be one of the main contributor to greenhouse gas emissions. The use of biobased materials, such as vegetal wools, is becoming increasingly relevant to meet the new thermal insulation expectations in buildings. Indeed, these materials present the advantage of storing carbon dioxide, which is the main greenhouse gas responsible for global warming, over a long period [1]. Moreover, these sustainable materials are in line with smart management of natural ressources having a lower environmental effect than traditional insulation materials [2].

On the other hand, vegetal wools are fibrous materials characterised by a strong variability at the level of their fibres such as their morphology, shape and size distribution [3–5]. These variabilities are related to the growing conditions [6] and the retting process [7], which corresponds to the first natural treatment of fibres. It reduces pectic cements and contributes to the mechanical defibration process [8]. To a certain extent the retted fibres present a better quality than the other unretted ones [9]. Thus, it seems that retting process does not modify the fibres size but allows an easier defibering process which leads to a better separation of fibre bundles [10,11].

* Corresponding author at: Cerema, Ifsttar, UMRAE – Laboratoire de Strasbourg, 11 rue Jean Mentelin, 67035 Strasbourg, France.
E-mail addresses: clement.piegay@cerema.fr (C. Piégay), philippe.gle@cerema.fr (P. Glé), emmanuel.gourdon@entpe.fr (E. Gourdon), etienne.gourlay@cerema.fr (E. Gourlay).

Despite these specificities, these materials have interesting thermal properties and have proven to be as efficient as conventional products [12]. Thermal conductivity values from the literature are summarized in the Table 1 for flax and hemp wools.

However, these values are slightly heterogeneous due to the different characterisation methods (permanent or transient operating conditions) and the hygrothermal conditions may also differ or are even not reported. Besides, vegetal wools have a strong hygroscopic behaviour [18], so that the hygrothermal conditions have a significant effect on their thermal conductivity. Ref. [13] highlights an increase of flax wool thermal conductivity of about 10% and of about 15% for hemp wool, when moisture increases from 0% to 10%. In [14] the impact of temperature on both flax and hemp thermal properties is also quantified. For a temperature increase of 10—30 °C, the thermal conductivity of these both material raises around 16%. This rise is also confirmed to a lesser extent in [19] for material based on palm fibres with thermal conductivity values of 0.0555 $W.m^{-1}.K^{-1}$ for 20 °C and 0.0578 $W.m^{-1}.K^{-1}$ for 30 °C.

Refs. [20,21] underlines that the thermal conductivity is also correlated to the material bulk density. Refs. [21–23] also specifies that the microstructural organisation and both the fibre composition and size have a strong impact on vegetal wool thermal properties.

Regarding modelling approaches, several models in the literature describe the thermal conductivity of porous media. A number of them have been evaluated for two fibrous material, a hemp wool [17] and a barkcloth material [24]. The relative deviations between experimental characterizations and modelling predictions are shown in the Table 2.

The commonly used basic models dedicated to biphasic media (including fluid and solid phases) are serie and parallel models [25]. In the first case, the heat flow passes successively through fluid phase and solid phase. This configuration gives a preponderant part to the fluid phase. In the second case, the heat flow passes through both fluid and solid phases all at once. A lot of other models are based on different mix of this two basic models such as the geometric model [26], Willye and Southwick model [27] and Krischer and Kröll model [28]. However, all these modelling approaches give high relative deviations with experimental measurements as shown in the Table 2. It can be explained by the fact that they have not been dedicated to the specific microstructure of materials. Willye and Southwick [27] and Krischer and Kröll [28] modelling approaches differ from the previous ones by taking the material anisotropic nature into account. However, their configuration cannot be adapted to take microscale parameters into account, such as fibre characteristics for fibrous materials.

Other models based on spherical geometries were also evaluated by these both papers. Halpin-Tsai model [29] and Lewis-Nielsen model [30] are dedicated to isotropic particles. They seem to underestimate the hemp wool thermal conductivity as shown in the Table 2. However, for the hemp fibres, the constituting repartition of each basic vegetal element (cellulose, hemicellulose, pectin and lignin) is different from that of hemp particles [34,35].

Table 2
Evaluation of thermal conductivity models based on relative deviation with experimental characterizations of a Hemp wool [17] and a Barkcloth material [24].

Model	Hemp wool [17]	Barkcloth material [24]	References
Serie	−38%	−66%	[25]
Parallel	+72%	−35%	[25]
Geometric	−26%	−51%	[26]
Willye & Southwick	(−17%)—(+60%)	/	[27]
Krisher & Kröll	(−32%)—(+15%)	/	[28]
Halpin-Tsai	−34%	/	[29]
Lewis-Nielsen	−24%	/	[30]
Maxwell solid spheres	/	−79%	[31]
Maxwell fluid spheres	+40%	/	[31]
Cheng & Vachon	/	−5%	[32]
SCM (2 phases)	+45%	/	[33]

Both Maxwell models with upper and lower limits are based on, respectively, dispersed solid spheres in a fluid phase and dispersed fluid spheres in a solid medium [31]. In the first case, Maxwell model underestimates the thermal conductivity value (relative deviation: 79%) and in the second case, it overestimates it (relative deviation: 40%). This can be explained by the fact that the modelling approach is based on an isotropic spherical geometry that is not adapted to the case of anisotropic fibrous materials closer to a cylindrical geometry.

Ref. [24] also evaluate the Cheng and Vachon model [32] which determines the effective thermal conductivity of a two phase solid mixture. With a relative deviation of 5%, this model is identified in [24] as the most suitable. However, as the other previous models, it is not specifically dedicated to the specific microstructure of fibrous materials.

In [17], the proposed model as the most suitable one is a numerical approach based on tomographic 3D images. Such a numerical approach had been previously developed by [36]. One of the main advantages of these methods is the relatively fine morphology modelling of the solid phase. However, these approaches require a large number of parameters and numerical calculations to build a 3D representative elementary volume. Moreover, even if the macroscopic properties of materials are based on microstructure parameters, there is no analytical relationships between them.

Other micro-macro approaches based on an analysis of the physical phenomena at the heterogeneities scale exist. A self-consistent method (SCM) has been used for instance by Boutin [33] based on the work carried out in [37]. It relies on an homogenisation between microscopic scale parameters and macroscopic scale properties. The specificity of this self-consistent approach is based on the energy equivalence between a generic inclusion representative of the physical and geometrical

Table 1
Thermal conductivity experimental values for flax and hemp wools.

Wool	Hygrothermal Conditions $T(°C)$ – $RH(\%)$	λ $\left(W.m^{-1}.K^{-1}\right)$	Density ρ_a $(kg.m^{-3})$	Regime	References
Flax	23 °C – 0%	0.0429	32	Permanent	[13]
	23 °C – 50%	0.065	25	Permanent	[14]
	/	0.052	27	Transient	[12]
Hemp	23 °C – 50%	0.062	25	Permanent	[14]
	/	0.037	100	Permanent	[15]
	/	0.04	/	/	[16]
	/	0.052	36.2	Transient	[12]
	room temp. –0%	0.047	/	Transient	[17]

properties of a media at microscopic scale, and the homogeneous equivalent medium at the macroscopic scale. However, the model proposed by Boutin [33] is dedicated to granular materials since it is based on an elementary volume with a spherical inclusion. As shown in the Table 2, this approach gives relatively far results from the experimental value with a relative deviation around 45%.

So, in order to better fit with vegetal fibres morphology and anisotropic material nature, it would be interesting to develop a similar self-consistent thermal conductivity modelling on the basis of a cylindrical inclusion. This approach can be validated by comparison with experimental data.

Thus, this paper is organised as follows: Section 2 introduces the studied materials used for modelling and the experimental device and methods used to characterise them. Then, Section 3 describes the thermal SCM model developed and used for vegetal wools. Finally, in Section 4, the model is validated by comparison with experimental data and both results and method used are discussed.

2. Materials and methods

In this section, four materials are first introduced. Then, the experimental method used to characterise the thermal conductivity is presented.

2.1. Materials

The four materials characterised for reference data are biobased fibrous materials. These vegetal wools are manufactured by a thermobinding process with only one type of vegetal fibre, hemp or flax. Both these fibre types have been chosen because they are among the most widely used vegetal fibres for building insulation. Materials are refered to "Hemp1", "Hemp2", "Flax1" and "Flax2". The first hemp wool stems ("Hemp1") were harvested with a retting period, but not the second one ("Hemp2"). For flax, both wools were retted, but the second one received an additional mechanical treatment to obtain a cottonized linen wool ("Flax2"). The four vegetal wools are shown in Fig. 1.

As a first approach, it appears that wools are made of successive horizontal and parallel fibre layers [38], which gives them an anisotropic behavior. These fibre layers are perpendicular to the heat flow in building applications.

The wools characteristics are presented in Table 3.

Both thickness and bulk density characterizations are based on 5 measurements for each material sample.

The four vegetal wools have been chosen to test the validity of the model developed in this paper. So, they present a different value range for bulk densities, thickness and porosities which enables us to analyse the influence of these parameters on the materials thermal conductivities.

2.2. Methods

2.2.1. Porosity

The porosity (ϕ) of these materials was determined thanks to the measurement protocol based on the works of Beranek [39] and optimised by Champoux et al. [40]. This direct caracterisation relies on the Boyle-Mariotte law. A known volume sample is placed in a hermetic and insulated cell to ensure isothermal measuring conditions. Then, a piston reduces the cell volume by a known value. The variation of pressure is measured by a differential pressure sensor. So, the solid phase volume can be determined using the Boyle-Mariotte law and thus, it enables to evaluate the sample open porosity. It corresponds to the inter-fibre and intra-fibre open porosity. In this work, the intra-fibre porosity is not considered.

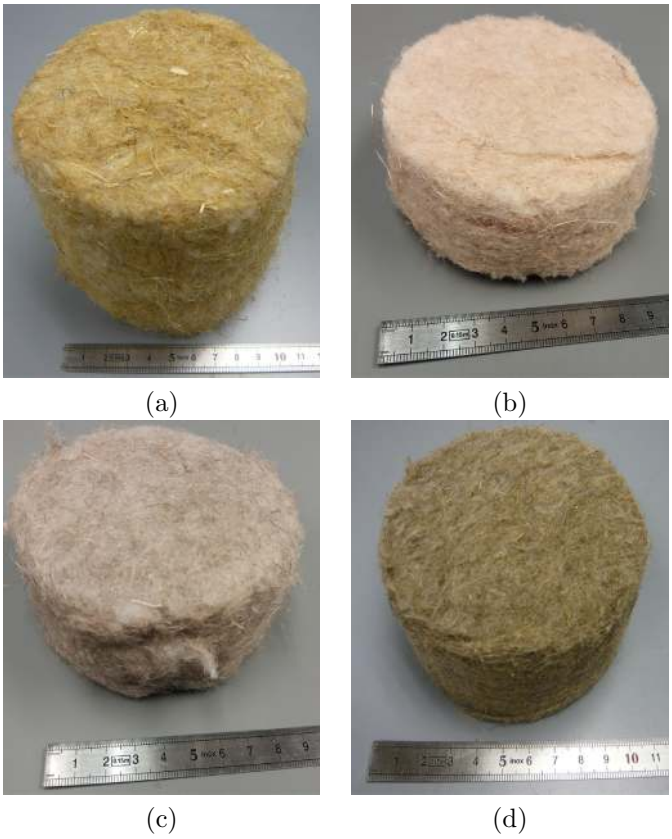

Fig. 1. The materials, (a) «Hemp1», (b) «Hemp2», (c) «Flax1», (d) «Flax2».

Table 3
Characteristics of the vegetal wools - Bulk density, porosity and thermal conductivity are obtained under the laboratory hygrothermal conditions ($T = 25 \pm 0.8\,^{\circ}\mathrm{C} - RH = 40 \pm 2\%$). Data are presented with mean value + standard deviation.

Material	Thickness (mm)	Bulk density ($kg.m^{-3}$)	Porosity (%)	Thermal conductivity ($mW.m^{-1}.K^{-1}$)
Hemp1	101 ± 2	45.4 ± 2.4	96.2 ± 0.2	44 ± 1
Hemp2	43 ± 1	67.2 ± 1.3	94.2 ± 0.2	55 ± 1
Flax1	50 ± 1	35.0 ± 1.8	97.5 ± 0.3	40 ± 2
Flax2	48 ± 2	66.3 ± 3.2	96.1 ± 0.3	50 ± 2

Indeed, it can be shown under simple assumptions that, for the range of studied materials porosities, the intra-fibre porosity is lower than 0.2% of the total porosity [4].

To determine this accessible porosity, measurements have been realised with 5 samples from each material under the laboratory hygrothermal conditions. Differences of 0.02% have been estimated between porosity values caracterized for relative humidities of 0% and 40%. This shows that moisture has a very low influence on accessible porosity. The results of this experimental characterisation are presented in Table 3. Generally, the vegetal wools porosity is very high with values above 90%. Moreover, the porosity range is directly correlated with the bulk density and the solid phase density.

2.2.2. Thermal conductivity

As vegetal wools are mainly used as insulating materials, thermal conductivity (λ) is evaluated to characterise their thermal properties.

Thermal conductivity measurements were made in the laboratory hygrothermal conditions, at a temperature of $T = 25 \pm 0.8\,^{\circ}\mathrm{C}$ and at a relative humidity of $RH = 40 \pm 2\%$.

The thermal conductivity of the materials was obtained by a transient measurement method. A Neotim FP2C © hot wire conductivimeter has been used. It is based on the Standard Test Method for Thermal Conductivity of Plastics by Means of a Transient Line Source Technique (ASTM D 5930-2017) and RILEM AAC 11-3 recommendation. With this device, a thermal shock probe is placed between two samples of the material to be characterised. The probe produces a local heating of a few degrees (above the ambient temperature). The temperature increase is recorded over time by the probe. The power sent by the probe is also known and when time tends to infinity, both these parameters could be related to sample thermal conductivity.

The experimental measurements have been performed with a power of 0.1 W and a measurement time of 120 s. For each test, the temperature increase is in the range $[15-20]\,^{\circ}$C. Ten thermal conductivity values have been obtained for each vegetal wools by varying the sample pairs and faces exposed to the probe.The experimental device, presented in Fig. 2(a), enables us to ensure an homogeneous contact between the probe and the samples. The thermal characterisation results of the four vegetal wools are presented in Table 3.

As expected, thermal conductivity values are correlated with bulk density and porosity values. For the same bulk density, the green hemp, which is the least porous material, has a higher thermal conductivity value than retted flax.

In order to extend the experimental thermal conductivity values to higher bulk densities, materials have been compressed. A one-dimensional compression along the axis perpendicular to the fibre layers and without impact on the fibres radii has been performed. In these conditions, the material thickness decreases without any significant modifications of other dimensions of the samples, as illustrated in Fig. 2.

Before the experimental measurement, a stabilisation time of five minutes has been respected to ensure the homogeneity of the samples under compaction. Experimental measurements are shown in Fig. 3.

These four wools present a similar behaviour with a linear increase of their thermal conductivity as a function of bulk density. Moreover, for a given bulk density (also check for porosity), «Hemp2» wool has the highest thermal conductivity, «Flax1» wool has the lowest one and both «Hemp1» and «Flax2» wools present equivalent values.

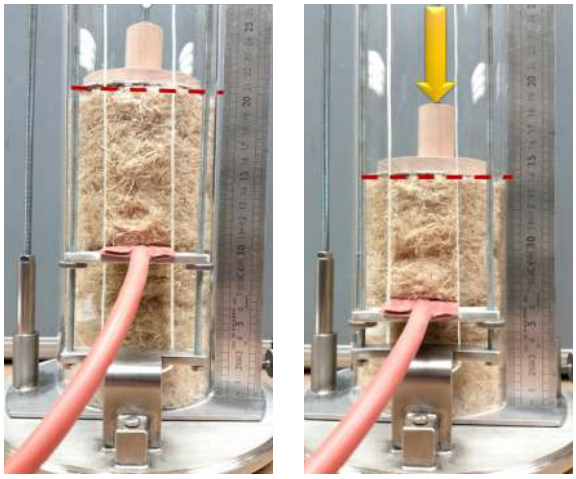

Fig. 2. Experimental compression device, (a) Hemp wool without compression (205 mm) (b) Hemp wool with compression (140 mm).

3. Modelling

Three types of heat transfer could be considered: convection, radiation and conduction.

Convection heat transfer has generally a negligible contribution in comparison with conduction effect according to several reference papers dealing with fibrous insulation materials. Indeed, for conventional fibrous insulation materials, this effect is not taken into account [22,41–44] as well as for vegetal fibrous insulation materials [23,16,45].

In [22,23,16,42–44], the heat transfer by radiation is expressed as a radiation conductivity, $\lambda_{radiation}$. Then, the equivalent material conductivity is determined by the sum of the conduction conductivity and the radiation conductivity. In a simple way, $\lambda_{radiation}$ can be expressed as a function of ρ^{-1}, the material bulk density. So, as shown in [22], the radiation effect for fibrous materials occurs for low bulk densities and its influence on the equivalent thermal conductivity is caracterized by an «optimum bulk density». For a material bulk density lower than this «optimum», the radiation heat transfer is the main effect and the thermal equivalent conductivity decrease quickly. For a material bulk density higher than this «optimum», the conduction heat transfer is the main effect and the thermal equivalent conductivity increases in a linear way.

For the studied vegetal wools, the experimental caracterisations, illustrated in Fig. 3, do not seem to show an «optimum bulk density» related on a radiation effect. However, based on the work

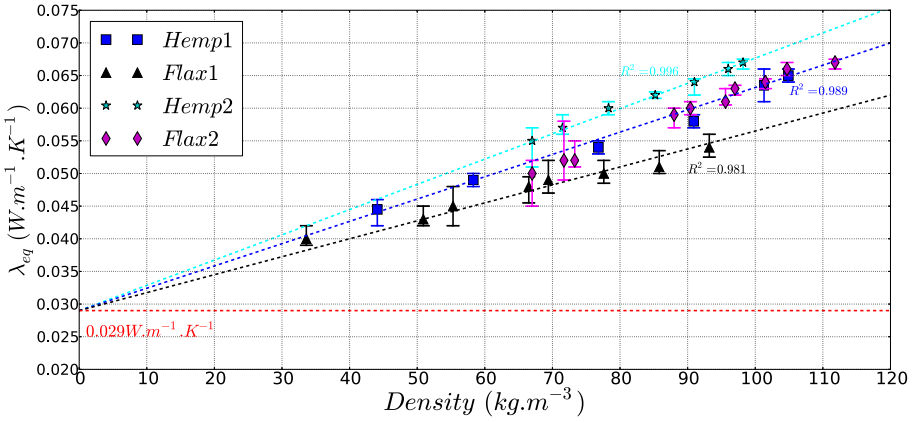

Fig. 3. Experimental measurements of vegetal wools thermal conductivities depending on the bulk density realised under the laboratory hygrothermal conditions ($T = 25\,^{\circ}$C – $RH = 40\%$).

leads by [22], we are aware that for the «Flax1» wool, having a bulk density of 35.0 kg.m^{-3}, we are at the limit of this radiation «optimum bulk density».

So, in this paper, the modelling approach is based on the equivalent thermal conductivity.

Moreover, in order to take microscopic parameters, such as fibres radii, into account, a micro-macro approach is used for the thermal conductivity modelling. One of these micro-macro methods is based on the homogenisation of periodic media (HPM) [46,47]. Thus, regardless of the microscopic geometry, it is possible to solve equations based on physical phenomena at micro scale by using numerical simulations. However, the aim of this paper is to obtained analytical equations of the effective thermal conductivity. So, a self-consistent method (SCM) can be used to find solutions in a simplified microscopic configuration at the fibres scale, but still representative of its specific morphology.

3.1. Hypotheses and basic principles of HPM

The homogenisation of periodic media is based on the following fundamental assumptions [46,47]: the existence of a representative elementary volume (REV) and the scale separation between the macroscopic media properties and the microscopic characteristics of heterogeneities.

So, the characteristic length (l) is related to the REV, as shown in Fig. 4, and the thermal phenomenon is associated to the macroscopic length (L). Both lengths are related to the scale ratio $\varepsilon = \frac{l}{L} \ll 1$.

This figure represents the simplified material modelling in which fibres are parallel to each other and in a regular layout.

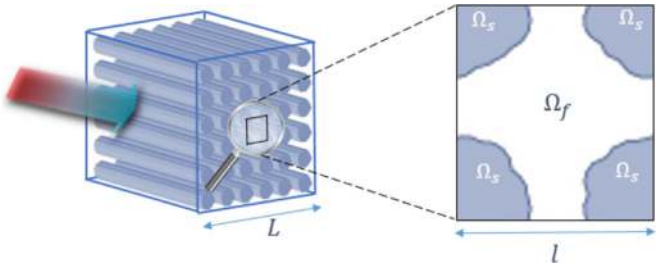

Fig. 4. The macroscopic porous medium (on the left) and the periodic cell of volume Ω at microscopic scale (on the right).

The case of a single porosity medium with a rigid skeleton is considered. As shown in Fig. 4, the medium is biphasic with a solid phase (Ω_s) satured by a fluid phase (Ω_f) composed of air. The air thermal conductivity is lower than the solid phase one. So, heat exchanges occur in the medium and at a local scale, the temperature variation (T) is ruled by the static linearised heat equation:

$$\lambda \Delta T + \overrightarrow{\text{grad}} T \,.\, \overrightarrow{\text{grad}} \lambda + m = \rho c \left(\frac{\partial T}{\partial t} \right) \tag{1}$$

m being the internal heat production and c the heat capacity.

The following assumptions can be made to simplify this equation:

- Small spatial variation of the specific thermal conductivity of each phase under a small temperature variation: $\overrightarrow{\text{grad}} \lambda = \vec{0}$;
- No internal heat production: $m = 0$;
- Permanent regime: $\frac{\partial T}{\partial t} = 0$

So, Eq. (1) becomes:

$$\lambda \Delta T = 0 \tag{2}$$

The last hypothesis of HPM concerns the energy consistency between the microscopic and macroscopic medium descriptions [48].

3.2. Basic configuration of SCM

Vegetal wools are natural fibrous insulation materials. So, to get a relevant simplified morphology of vegetal wools microstructure, we consider here a generic cylindrical inclusion at the fibre scale as a representative volume (Ω), described by radius (R) and surface ($\partial\Omega$). This volume matches an inclusion of a fluid cylinder having a radius βR and a volume Ω_f, into a solid cylinder of radius R and volume Ω_s, as shown in Fig. 5. Thus, the porosity of this inclusion is $\phi = \frac{\Omega_f}{\Omega} = \beta^2$. Since the solid phase is composed of vegetal fibres but also of polymer fibres (generally around 15% of vegetal wools mass), an average radius based on the distributions of these two types of fibres is considered for this phase [5].

Moreover, in a first approach, the effect related to contact resistance between fibres, discussed in [49], was not taken into account. However, we are aware that it could have an impact on the modelling results. In this paper, the hypothesis of a perfect contact between the fibres is done. The thermal contact conductance

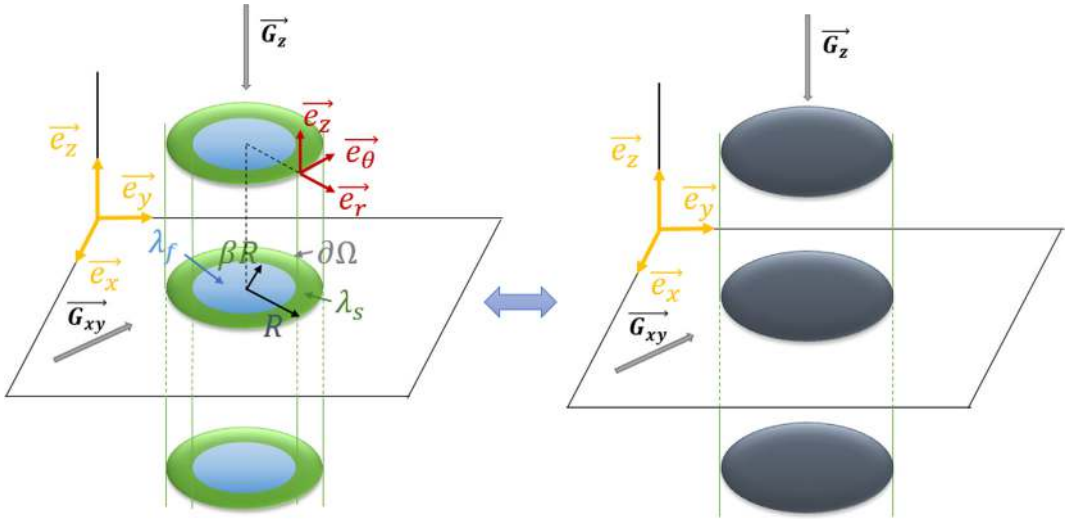

Fig. 5. The generic solid-fluid inclusion (on the left) and the equivalent macroscopic medium (on the right).

constant (C), introduced in [49] to take the contact between the fibres into account in a generalized self-consistent spherical modelling approach, tends towards infinity and the additional term to $\frac{1}{C}$ tends towards 0.

As for HPM, the behaviour of both equivalent macroscopic media and corresponding phases complies with heat equation given in Eq. (2). The aim is to find an equation between the effective thermal conductivity (at the macro scale), the specific thermal conductivity of each phase and the porosity (at the micro scale). So, the hypothesis made here is that the equivalent macroscopic medium and the generic fluid-solid inclusion are both submitted to a uniform forcing temperature gradient ($\vec{G}$), with $\vec{G} = \overrightarrow{\text{grad}}\, T$, as shown in Fig. 5. $\vec{G}$ is characterised by an amplitude (G) and a direction.

The fibre organisation in the material depends on the manufacturing process. So, as underlined previously (cf. paragraph 2.1.), vegetal wools panels have fibres organised in parallel layers. Due to this vegetal wools anisotropy, we can define two main working directions. The first one is perpendicular to the fibre direction and is based on $\left(\vec{e_r}, \vec{e_\theta}\right)$ plane. The second one is parallel to the fibres according to the $\vec{e_z}$ axis, as shown in Fig. 5. However, only the first case corresponds to the main practical orientation of these insulation materials. In these conditions, even if all scenarios could exist, only one specific modelling case is studied: the thermal flow perpendicular to the fibres.

3.3. SCM approach for a perpendicular heat flow

In the rest of this paper, the index *s*, *f* and *eq* correspond respectively to the solid and fluid phases and to the equivalent macroscopic medium. In the following subsection, the index α can be replaced by each of previously index (*s*, *f* and *eq*).

3.3.1. Temperature expression

The heat equation, Eq. (2), can be written in cylindrical coordinates:

$$\frac{\partial^2 T_\alpha}{\partial r^2} + \frac{1}{r}\frac{\partial T_\alpha}{\partial r} + \frac{1}{r^2}\frac{\partial^2 T_\alpha}{\partial \theta^2} = 0 \tag{3}$$

To find generic solution of Eq. (4), temperature can be written with two independent functions: $T_\alpha(r,\theta) = f_\alpha(r).h(\theta)$. In view of the hypothesis, $h(\theta)$ can be written as:

$$h(\theta) = G\sin(\theta) \tag{4}$$

$T_\alpha(r,\theta)$ becomes:

$$T_\alpha(r,\theta) = G f_\alpha(r)\sin(\theta) \tag{5}$$

Using Eq. (5) into Eq. (3), we obtain a classical second order differential equation:

$$f''_\alpha(r) + \frac{1}{r}f'_\alpha(r) - \frac{1}{r^2}f_\alpha(r) = 0 \tag{6}$$

Which solution is:

$$f_\alpha(r) = A_\alpha r + \frac{1}{r}B_\alpha \tag{7}$$

A_α and B_α being two constants.

Eq. (5) becomes:

$$T_\alpha(r,\theta) = G\left(A_\alpha r + \frac{1}{r}B_\alpha\right)\sin(\theta) \tag{8}$$

3.3.2. Boundary conditions

The aim of this section is to determine the constants related to the fluid phase, the solid phase and the equivalent macroscopic medium.

In the fluid phase, $0 < r \leqslant \beta R$:

$$T_f(r,\theta) = G\left(A_f r + \frac{1}{r}B_f\right)\sin(\theta) \tag{9}$$

In the specific case where $r = 0$, the temperature has a finite value, so $B_f = 0$. Eq. (9) becomes:

$$T_f(r,\theta) = GA_f r\sin(\theta) \tag{10}$$

In the solid phase, $\beta R \leqslant r \leqslant R$:

$$T_s(r,\theta) = G\left(A_s r + \frac{1}{s}B_f\right)\sin(\theta) \tag{11}$$

At the fluid/solid interface, $r = \beta R$, we consider both temperature and heat flow continuity:

$$A_f \beta R = A_s \beta R + \frac{B_s}{\beta R} \tag{12}$$

$$\lambda_f A_f = \lambda_s^\perp \quad A_s - \frac{B_s}{(\beta R)^2}\Bigg) \tag{13}$$

We also consider this continuity at $r = R$, the interface between solid phase and equivalent macroscopic medium:

$$A_s R + \frac{B_s}{R} = A_{eq}R + \frac{B_{eq}}{R} \tag{14}$$

$$\lambda_s^\perp\left(A_s - \frac{B_s}{R^2}\right) = \lambda_{eq}^\perp\left(A_{eq} - \frac{B_{eq}}{R^2}\right) \tag{15}$$

When r becomes very high and tends to infinity: $\vec{G} = \overrightarrow{\text{grad}}T$. So, we can write for $\vec{e_r}$ axis:

$$G\left(A_{eq} - \frac{B_{eq}}{r^2}\right) = G \tag{16}$$

with $r \to +\infty$, we have: $A_{eq} = 1$

The last boundary condition is the energy consistency. It is represented by the equality of the integration of temperature gradient over its volume without the cylindrical inclusion and with the cylindrical inclusion:

$$\int_\Omega \overrightarrow{\text{grad}}T(r,\theta)\text{d}\Omega = \int_\Omega \overrightarrow{\text{grad}}T_{eq}(r,\theta)\text{d}\Omega \tag{17}$$

$$G\Omega = G\Omega\left(1 - \frac{B_{eq}}{R^2}\right) \tag{18}$$

So, $B_{eq} = 0$

Eqs. (14) and (15) becomes:

$$A_s R + \frac{B_s}{R} = R \tag{19}$$

$$\lambda_s^\perp\left(A_s - \frac{B_s}{R^2}\right) = \lambda_{eq} \tag{20}$$

We have a four equation system, Eqs. (12), (13), (19) and (20), and three unkown constants. The resolution of this system leads to the equivalent thermal conductivity expressed as a function of thermal conductivities of both phases and material porosity:

$$\lambda_{eq}^\perp = \lambda_s^\perp\left(1 + \frac{\phi}{\frac{(1-\phi)}{2} + \frac{1}{\frac{\lambda_f}{\lambda_s^\perp} - 1}}\right) \tag{21}$$

4. Validation and discussion

In this section, the developed SCM model is validated by comparison with experimental measurements. In this approach, it is

therefore necessary to use values of both solid and fluid phases thermal conductivities. So, first of all, values of both solid and fluid phases thermal conductivities are presented. Then, it is possible to use this cylindrical SCM model to optimise vegetal wools thermal performances by varying some of their parameters. Finally, the global approach used to determine thermal conductivity is discussed.

4.1. Solid and fluid phases parameters

In order to determine the equivalent thermal conductivity, both solid and fluid phases thermal conductivity should be known.

Fig. 3, previously presented, shows equivalent thermal conductivity values of the four studied materials depending on bulk density. When bulk density tends towards zero, the equivalent thermal density tends towards fluid phase thermal conductivity. Then, based on data presented in Fig. 3, a linear extrapolation is done.

So, a mean equivalent value equal to $\lambda_f = 0.029\ \mathrm{W.m^{-1}.K^{-1}}$ is determined. As experimental measurements are realised in laboratory hygrothermal conditions, this value is a little higher than the dry air thermal conductivity. This value will be used in the rest of this paper.

For the solid phase, only a few data about vegetal fibres are available in the literature. Ref. [50] gives a hemp thermal conductivity value of $\lambda_s = 0,58\ \mathrm{W.m^{-1}.K^{-1}}$ based on a model inversion from hemp particle. However, as mentioned above, the constituting repartition of each basic vegetal element (cellulose, hemicellulose, pectin and lignin) is different between hemp fibers and hemp particles [34,35]. Ref. [17] uses also a hemp thermal conductivity value of $\lambda_s = 0,44\ \mathrm{W.m^{-1}.K^{-1}}$ which comes originally from a work carried out on wood [51]. However, Thunman and Leckner [52] give a perpendicular thermal conductivity value of $0,52\ \mathrm{W.m^{-1}.K^{-1}}$ for a dry wood fibre and Saastamoinen & Richard [53] suggest a value of $0,6\ \mathrm{W.m^{-1}.K^{-1}}$. In this case too, the constituting percentage of each basic vegetal element of both hemp and wood fibres are different [54,55]. However, the fibre nature has a high influence on the solid phase thermal conductivity [21]. Moreover, the chemical composition of vegetal fibres also has an impact on their both sensitivity and behaviour towards moisture [56].

Due to the lack of clearly established data for these materials, the solid phase thermal conductivity has been determined in this paper by a model inversion, as it is usually done in the literature [25,33,57,37,58]. In order to estimate the perpendicular conductivities of the solid phases for each studied materials, we used the SCM model which is based on a geometry close to vegetal fibres. Values are presented in Table 4.

They are close to each other, with a deviation range of $0.12\ \mathrm{W.m^{-1}.K^{-1}}$. These values are in the same range than those presented above for both wood and hemp fibres. So, the solid phase thermal conductivities estimated in this paper can be considered as acceptable values and they will be used in the following part of this paper.

Table 4
Solid phase thermal conductivity of studied materials.

Material	$\lambda_s^{\perp}$ ($\mathrm{W.m^{-1}.K^{-1}}$)
Hemp	0.72
Green hemp	0.78
Flax	0.66
Retted flax	0.73

4.2. Modelling validation

The aim of this section is to validate the developed cylindrical SCM model by comparison with experimental measurements.

To do that, graphs representing the modelling and the experimental data for each studied vegetal wool are presented in Fig. 6. Each experimental data is represented by a mean value and both the max and min values. For the four materials, the developed SCM model provides good results. The modellings fit well the experimental data and stand in the experimental range, except for three values. The first one for hemp wool and the second and third for retted flax wool. To estimate the corresponding gaps, the relative deviation between modelling values and experimental data is calculated and presented in Table 5.

For the four wools, the mean relative deviations are lower than 2%. All of the maximum values of the relative deviations are lower than 5%.

It is also possible to assess the cylindrical SCM modelling approach on the basis of literature data, such as those presented

Table 5
The mean, max and min relative deviations between modelling values and experimental data of studied materials.

Material	Mean relative deviation (%)	Min of relative deviation (%)	Max of relative deviation (%)
Hemp	1.3	0.2	3.1
Green hemp	0.4	0	1.0
Flax	1.3	0.6	2.5
Flax retted	1.8	0.2	4.8

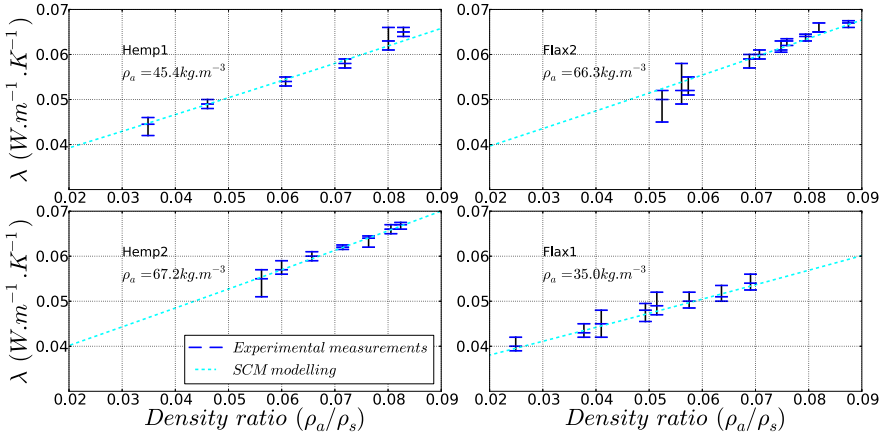

Fig. 6. Comparison between thermal conductivity modelled with the cylindrical SCM approach and experimental data.

in Table 1. However, to do this, data related to the material porosity and the solid phase thermal conductivity are necessary. In [17] all these data are available for a hemp wool. In the other references we have only a material density value, so that both porosity and solid phase thermal conductivity values must be determined. So, only an indicative value of equivalent thermal conductivity can be determined. Results are presented in the Table 6.

So, these results indicate that the SCM approach developed here can be validated in order to model thermal conductivity of vegetal wools.

4.3. Analysis of parameters influencing the vegetal wools thermal performances

Now, on the basis of this model, it is possible to analyse the influence of various parameters on the thermal performances of vegetal wools. To do this, it is possible to vary both solid phase thermal conductivity and porosity. The variation of these parameters have been chosen to simulate materials as close as possible to vegetal wools used for bulding insulation. So, the parameters vary in the following ranges:

- λ_s in [0.4–0.8] $W.m^{-1}.K^{-1}$ with a step of 0.01 $W.m^{-1}.K^{-1}$,
- ϕ in [0.8–1] with a step of 0.01.

Results are presented in Fig. 7.

For a porosity value higher than 95%, the equivalent thermal conductivity of the material is very interesting for building insulation even if the solid phase thermal conductivity is high. For example, with a porosity value of 97% and a solid phase thermal conductivity of 0.72 $W.m^{-1}.K^{-1}$, it is possible to obtain an equivalent thermal conductivity equal to 0.04 $W.m^{-1}.K^{-1}$, as illustrated in Fig. 7.

4.4. Discussion about future outlooks and validity limits of the model

In the case of a heat flow perpendicular to vegetal wools, the determination of the equivalent thermal conductivity by the SCM approach has been validated by comparing it with experimental measurements. However, the range of the ratio between bulk density and solid phase density used for this validation stays relatively limited with a maximum value lower than 0.1, but it already represents a high compression ratio that is difficult to achieve under conventional operating conditions. Indeed, the strains endured by vegetal wools during their packaging and their implementation are related to the density ratio range used to validate the SCM approach. So, for a conventional use of vegetal wools, the SCM approach based on a cylindrical geometry seems to be adapted to determine their equivalent thermal conductivity. This has been verified with using the modelling approach based on literature data. Unlike other modelling approaches, it is based on a simplified representative elementary volume close to the vegetal fibres microstructural morphology. However, in this paper no parameters related to contact resistance between fibres have been taken into account. So, to improve the cylindrical SCM approach it could be relevant to introduce this effect on the basis of the generalized self-consistent modelling approach used in [49].

Moreover to the knowledge of authors, no experimental data concerning hemp or flax fibres thermal conductivities are available in the literature. For this reason, this parameter has been determined here as in previous works by inversion of the model. This is a limit of the SCM approach in the case of vegetal fibrous materials. It can be mitigated by the fact that for a porosity higher than 95%, thermal conductivity does not really depend on the solid phase thermal conductivity as shown by the Fig. 7. Indeed, an equivalent thermal conductivity value around 0.04 $W.m^{-1}.K^{-1}$ can be obtained regardless of the solid phase thermal conductivity.

Table 6
Equivalent cylindrical SCM thermal conductivity based on reference literature data.

Wool	Exp. λ $\left(W.m^{-1}.K^{-1}\right)$	SCM $\lambda_{eq}^{\perp}$ $\left(W.m^{-1}.K^{-1}\right)$	Relative deviation (%)	References
Flax	0.0429	0.0442	3.0	[13]
	0.065	0.0664	2.1	[14]
	0.052	0.0535	2.8	[12]
Hemp	0.062	0.0635	2.4	[14]
	0.052	0.0533	2.5	[12]
	0.047	**0.0466**	**0.9**	[17]

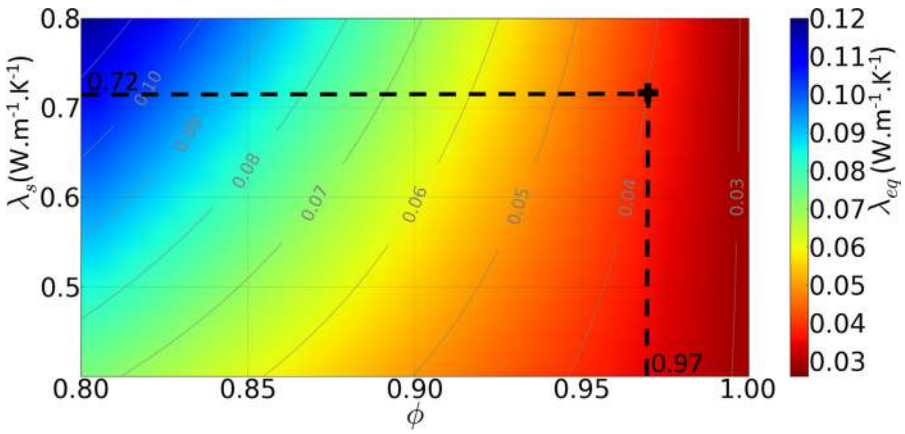

Fig. 7. Modelling of the equivalent thermal conductivity of a vegetal wool with the SCM approach as a function of porosity range and solid phase thermal conductivity.

Thus, as it is difficult to characterise the solid phase thermal conductivity in the case of vegetal fibrous materials, this is an interesting result. So, the parametric analysis has shown that better equivalent thermal conductivity of vegetal wools can be obtained by minimising the density to obtain an optimal porosity. However, we must keep in mind, that for low density values, the radiation effect can disturb the equivalent thermal conductivity.

The solid phase thermal conductivities obtained by SCM modelling inversion seem to be high by comparing them with literature values. So, it would be interesting to compare these results with experimental data realised on both hemp and flax fibres. As it is very difficult to experimentally characterise this microstructural parameter, an investigation could be based on the thermal conductivity of each chimical component (hemicellulose, cellulose, pectin and lignin).

Finally, a focus has been made on the specific case of a perpendicular flow, but it would also be particularly relevant to investigate a modelling approach based on mix of both perpendicular and parallel flows. Indeed, due to the manufacturing process, the fibres are not always placed in regular parallel layers and can present a slight inclination [38].

5. Conclusion

Biobased materials are increasingly used for greenbuilding insulation. In this context, it is interesting to develop a micro-macro modelling approach to predict the equivalent thermal conductivity of vegetal wools. Indeed, considering the microstructural specificities of these fibrous materials, it is particulary relevant to connect both microscale parameters and macroscale properties. To do this, it is possible to develop a cylindrical self-consistent modelling based on a representative elementary volume with a cylindrical geometry much closer to fibres than other more conventional and more common models. Moreover, this model is based on only two parameters related to material microstructure: the solid phase thermal conductivity (λ_s) and the porosity (ϕ) in which the mean radius of the solid phase is included.

In this paper, this cylindrical SCM approach has been validated by comparison with experimental characterisations performed on four materials in real hygrothermal conditions and with data from literature.

Then, in order to promote the greenbuilding field with thermal performances close to those of conventional materials, the influence of parameters such as porosity or solid phase conductivity value on the vegetal wools thermal properties has been analysed. So, it has been shown that for a porosity higher than 95%, an interesting equivalent thermal conductivity value can be obtained regardless of the solid phase thermal conductivity, which is very difficult to characterise experimentally.

Finally, in order to extend this modelling approach based on a specific perpendicular flow, future work will investigate other flow orientations. Another development will also be made to integrate contact resistance between the fibres in the cylindrical SCM approach.

Declaration of Competing Interest

The authors declare that they have no known competing financial interests or personal relationships that could have appeared to influence the work reported in this paper.

Acknowledgements

This work was performed within the framework of the LABEX CeLyA (ANR-10-LABX-0060) of Université de Lyon, France. Moreover, the authors thank the Laroche S.A. company and the CAVAC Biomatériaux company for providing them the materials of this study. The authors also thank Sandrine Marceau, Ifsttar, MAST/CPDM of Université Paris-Est, for helping them in the analysis of vegetal wools microstructure.

References

[1] G. Lumia, Bio-based insulation materials: an opportunity for the renovation of European residential building stock. Evaluation of carbon uptake benefits through a dynamic life cycle assessment (DLCA) (Ph.D. thesis), 2017..
[2] F. Asdrubali, S. Schiavoni, K. Horoshenkov, A review of sustainable materials for acoustic applications, Building Acoustics 19 (4) (2012) 283–312.
[3] K.V. Horoshenkov, K. Attenborough, S.N. Chandler-Wilde, Padé approximants for the acoustical properties of rigid frame porous media with pore size distributions, J. Acoust. Soc. Am. 104 (3) (1998) 1198–1209, https://doi.org/10.1121/1.424328. URL: http://asa.scitation.org/doi/10.1121/1.424328.
[4] P. Glé, Acoustics of building materials based on plant fibers and particules: tools for characterization, modelling and optimisation, INSA de Lyon, 2013 (Ph. D. thesis).
[5] C. Piégay, P. Glé, E. Gourdon, E. Gourlay, S. Marceau, Acoustical model of vegetal wools including two types of fibers, Appl. Acoust. 129 (2018) 36–46, https://doi.org/10.1016/j.apacoust.2017.06.021. URL: http://linkinghub.elsevier.com/retrieve/pii/S0003682X17303274.
[6] A. Tomsen, S. Rasmussen, V. Bohn, K. Nielsen, A. Thygesen, Hemp raw materials: the effect of cultivar, growth conditions and pretreatment on the chimical composition of fibres, Riso National Laboratory, Riso-R-1507(EN)..
[7] B. Pallesen, The quality of combine-harvested fibre flax for industrials purposes depends on the degree of retting, Ind. Crops Prod. 5 (1) (1996) 65–78.
[8] P. Bouloc, Le chanvre industriel: production et utilisations, editions france agricole Edition, 2006..
[9] R. Hobson, D. Hepworth, D. Bruce, Quality of fibre separted from unretted hemp stems by decortication, J. Agric. Eng. Res. 78 (2) (2001) 153–158, https://doi.org/10.1006/jaer.2000.0631.
[10] V. Placet, A. Day, J. Beaugrand, The influence of unintended field retting on the physicochemical and mechanical properties of industrial hemp bast fibres, J. Mater. Sci. 52 (10) (2017) 1–19, https://doi.org/10.1007/s10853-017-0811-5.
[11] B. Mazian, A. Bergeret, J.-C. Benezet, L. Malhautier, Influence of field retting duration on the biochemical, microstructural, thermal and mechanical properties of hemp fibres harvested at the beginning of flowering, Ind. Crops Prod. 116 (2018) 170–181.
[12] M. Volf, J. Divis, F. Havlík, Thermal, moisture and biological behaviour of natural insulating materials, Energy Procedia 78 (2015) 1599–1604, https://doi.org/10.1016/j.egypro.2015.11.219. URL: https://linkinghub.elsevier.com/retrieve/pii/S1876610215019517.
[13] A. Korjenic, V. Petránek, J. Zach, J. Hroudová, Development and performance evaluation of natural thermal-insulation materials composed of renewable resources, Energy Build. 43 (9) (2011) 2518–2523, https://doi.org/10.1016/j.enbuild.2011.06.012. URL: http://linkinghub.elsevier.com/retrieve/pii/S0378778811002611.
[14] A. Korjenic, J. Zach, J. Hroudová, The use of insulating materials based on natural fibers in combination with plant facades in building constructions, Energy Build. 116 (2016) 45–58, https://doi.org/10.1016/j.enbuild.2015.12.037. URL: http://linkinghub.elsevier.com/retrieve/pii/S0378778815304722.
[15] A. Kremensas, R. Stapulionien, S. Vaitkus, A. Kairyt, Investigations on physical-mechanical properties of effective thermal insulation materials from fibrous hemp, Proc. Eng. 172 (2017) 586–594, https://doi.org/10.1016/j.proeng.2017.02.069. URL: http://linkinghub.elsevier.com/retrieve/pii/S1877705817305751.
[16] A. Tilioua, L. Libessart, A. Joulin, S. Lassue, B. Monod, G. Jeandel, Determination of physical properties of fibrous thermal insulation, EPJ Web Conf. 33 (2012) 02009, https://doi.org/10.1051/epjconf/20123302009. URL: http://www.epj-conferences.org/10.1051/epjconf/20123302009.
[17] R. El-Sawalhi, J. Lux, P. Salagnac, Estimation of the thermal conductivity of hemp based insulation material from 3d tomographic images, Heat Mass Transf. 52 (8) (2016) 1559–1569, https://doi.org/10.1007/s00231-015-1674-4. URL: http://link.springer.com/10.1007/s00231-015-1674-4.
[18] F. Collet, M. Bart, L. Serres, J. Miriel, Porous structure and water vapour sorption of hemp-based materials, Constr. Build. Mater. 22 (6) (2008) 1271–1280, https://doi.org/10.1016/j.conbuildmat.2007.01.018. URL: http://linkinghub.elsevier.com/retrieve/pii/S0950061807000396.
[19] K. Manohar, Renewable building thermal insulation – oil palm fibre, Int. J. Eng. Technol. 2 (3) (2012) 475–479.
[20] Z. Ye, C.M. Wells, C.G. Carrington, N.J. Hewitt, Thermal conductivity of wool and wool-hemp insulation, Int. J. Energy Res. 30 (1) (2006) 37–49, https://doi.org/10.1002/er.1123. http://doi.wiley.com/10.1002/er.1123.
[21] R. Stapulionien, S. Vaitkus, S. Vjelis, A. Sankauskait, Investigation of thermal conductivity of natural fibres processed by different mechanical methods, Int. J. Precis. Eng. Manuf. 17 (10) (2016) 1371–1381, https://doi.org/10.1007/s12541-016-0163-0. URL: http://link.springer.com/10.1007/s12541-016-0163-0.
[22] C. Bankvall, Heat transfer in fibrous materials, J. Test. Eval. 1 (3) (1973) 235–243, https://doi.org/10.1520/JTE10010.

[23] J. Finck, Mechanism of heat flow in fibrous materials, Bureau Stand. J. Res. 6 (1930) 973–984.
[24] S. Rwawiire, B. Tomkova, J. Militky, L. Hes, B.M. Kale, Acoustic and thermal properties of a cellulose nonwoven natural fabric (barkcloth), Appl. Acoust. 116 (2017) 177–183, https://doi.org/10.1016/j.apacoust.2016.09.027. URL: http://linkinghub.elsevier.com/retrieve/pii/S0003682X1630305X.
[25] V. Cérézo, Propriétés mécaniques, thermiques et acoustiques d'un matériau à base de particules végétales: approche expérimentale et modélisation théorique, Ecole Nationale des Travaux Publics de l'Etat, 2005 (Ph.D. thesis) http://theses.insa-lyon.fr/publication/2005isal0037/these.pdf.
[26] K. Lichtenecker, Der elektrische Leitungswiderstand künstlicher und natürlicher Aggregate, Physikalische Zeitschrift 25 (1924). 169–181,193–204,226–233.
[27] M. Wyllie, P. Southwick, An experimental investigation of the s.p. and resistivity phenomena in dirty sands, J. Petrol. Technol. 6 (02) (1954) 44–57, https://doi.org/10.2118/302-G.
[28] O. Krischer, K. Kroll, Die wissenschaftlichen Grundlagen der Trocknungstechnik, springer verlag berlin Edition, 1956..
[29] R.K. Goyal, A.N. Tiwari, Y.S. Negi, Microhardness of PEEK/ceramic micro-and nanocomposites: correlation with Halpin-Tsai model, Mater. Sci. Eng.: A 491 (1–2) (2008) 230–236.
[30] R. Pal, On the Lewis-Nielsen model for thermal/electrical conductivity of composites, Compos. Part A: Appl. Sci. Manuf. 39 (5) (2008) 718–726.
[31] J.C. Maxwell, A treatise on electricity and magnetism, Clarendon Press I (1873) 598.
[32] S. Cheng, R. Vachon, The prediction of the thermal conductivity of two and three phase solid heterogeneous mixtures, Int. J. Heat Mass Transf. 12 (1969) 249–264.
[33] C. Boutin, Conductivité thermique du béton cellulaire autoclavé: modélisation par méthode autocohérente, Matériaux et Constructions 29 (6) (1996) 609–615, https://doi.org/10.1007/BF02485968.
[34] P.H.F. Pereira, M.d.F. Rosa, M.O.H. Cioffi, K.C.C.d.C. Benini, A.C. Milanese, H.J.C. Voorwald, D.R. Mulinari, Vegetal fibers in polymeric composites: a review, Polímeros 25 (1) (2015) 9–22, https://doi.org/10.1590/0104-1428.1722.
[35] G. Delannoy, Durabilité d'isolants á base de granulats végétaux, Université Paris-Est, 2018 (Ph.D. thesis).
[36] J. Lux, A. Ahmadi-Sénichault, C. Gobbé, C. Delisée, Macroscopic thermal properties of real fibrous materials: volume averaging method and 3d image analysis, Int. J. Heat Mass Transf. 49 (11) (2006) 1958–1973, https://doi.org/10.1016/j.ijheatmasstransfer.2005.09.038.
[37] Z. Hashin, Assessment of the self consistent scheme approximation: conductivity of particulate composites, J. Compos. Mater. 2 (3) (1968) 284–300, https://doi.org/10.1177/002199836800200302.
[38] L. Lei, N. Dauchez, J. Chazot, Prediction of the six parameters of an equivalent fluid model for thermocompressed glass wools and melamine foam, Appl. Acoust. 139 (2018) 44–56, https://doi.org/10.1016/j.apacoust.2018.04.010. URL: https://linkinghub.elsevier.com/retrieve/pii/S0003682X17305728.
[39] L. Beranek, Acoustic impedance of porous materials, J. Acoust. Soc. Am. 13 (1942) 248–260.
[40] Y. Champoux, M.-R. Stinson, G.-A. Daigle, Air-based system for the measurement of porosity, J. Acoust. Soc. Am. 89 (2) (1991) 910–916.
[41] M. Bomberg, S. Klarsfeld, Semi-empirical model of heat transfer in dry mineral fiber insulations, J. Therm. Insul. 6 (3) (1983) 156–173.
[42] S. Bories, Natural convection in porous media, in: M. Corapcioglu, J. Bear (Eds.), Advances in Transport Phenomena in Porous Media, Springer, Dordrecht, 1987, https://doi.org/10.1007/978-94-009-3625-64.
[43] A. Karamanos, A. Papadopoulos, D. Anastasellos, Heat transfer phenomena in fibrous insulating materials, in: Proceedings of, 2004..
[44] R. Ji, Z. Zhang, L. Liu, X. Wang, Development of the random simulation model for estimating the effective thermal conductivity of insulation materials, Build. Environ. 80 (2014) 221–227, https://doi.org/10.1016/j.buildenv.2014.05.033. URL: http://linkinghub.elsevier.com/retrieve/pii/S0360132314001838.
[45] J. Lux, Comportement thermique macroscopique de milieux fibreux réels anisotropes: étude basée sur l'analyse d'images tridimensionnelles, Université Sciences et Technologies-Bordeaux I, 2005 (Ph.D. thesis).
[46] J.L. Auriault, Dynamic behaviour of a porous medium saturated by a newtonien fluid, Int. J. Eng. Sci. 18 (6) (1980) 775–785, https://doi.org/10.1016/0020-7225(80)90025-7.
[47] E. Sanchez-Palencia, Non-homogeneous Media and Vibration Theory, Springer-Verlag, Berlin, 1980.
[48] C. Boutin, C. Geindreau, Estimates and bounds of dynamic permeability of granular media, J. Acoust. Soc. Am. 124 (6) (2008) 3576–3593, https://doi.org/10.1121/1.2999050. URL: http://asa.scitation.org/doi/10.1121/1.2999050.
[49] Y.-M. Lee, R.-B. Yang, S.-S. Gau, A generalized self-consistent method for calculation of effective thermal conductivity of composites with interfacial contact conductance, Int. Commun. Heat Mass Transfer 33 (2) (2006) 142–150, https://doi.org/10.1016/j.icheatmasstransfer.2005.10.004. URL: https://linkinghub.elsevier.com/retrieve/pii/S073519330500196X.
[50] S. Nguyen, A. Tran-Le, M. Vu, Q. To, O. Douzane, T. Langlet, Modeling thermal conductivity of hemp insulation material: a multi-scale homogenization approach, Build. Environ. 107 (2016) 127–134, https://doi.org/10.1016/j.buildenv.2016.07.026. URL: http://linkinghub.elsevier.com/retrieve/pii/S0360132316302815.
[51] J.F. Siau, Transport Processes in Wood, springer – verlag Edition, Springer Series in Wood Science, T.E. Timell, 1984..
[52] Bo Leckner, H. Thunman, Thermal conductivity of wood – models for different stages of combustion, Biomass Bioenergy (23) (2002) 47–54. oCLC: 925715613.
[53] J. Saastamoinen, J.-R. Richard, Simultaneous drying and pyrolysis of solid fuel particules, Combust. Flame 106 (1996) 288–300.
[54] M.R. Vignon, C. Garcia-Jaldon, D. Dupeyre, Steam explosion of woody hemp chenevotte, Int. J. Biol. Macromol. 17 (6) (1995) 395–404.
[55] J. Eitelberger, K. Hofstetter, Prediction of transport properties of wood below the fiber saturation point – a multiscale homogenization approach and its experimental validation, Compos. Sci. Technol. 71 (2) (2011) 134–144, https://doi.org/10.1016/j.compscitech.2010.11.007. URL: http://linkinghub.elsevier.com/retrieve/pii/S0266353810004264.
[56] C.A.S. Hill, A. Norton, G. Newman, The water vapor sorption behavior of natural fibers, J. Appl. Polym. Sci. 112 (3) (2009) 1524–1537, https://doi.org/10.1002/app.29725. URL: http://doi.wiley.com/10.1002/app.29725.
[57] E. Gourlay, Caractérisation expérimentale des propriétés mécaniques et hygrothermiques du béton de chanvre, ENTPE, 2014 (Ph.D. thesis).
[58] F. Collet, S. Pretot, Thermal conductivity of hemp concretes: Variation with formulation, density and water content, Constr. Build. Mater. 65 (2014) 612–619, https://doi.org/10.1016/j.conbuildmat.2014.05.039. URL: https://linkinghub.elsevier.com/retrieve/pii/S0950061814005224.